Spectral and Time Phenomena in Optical Injection Using Distributed Feedback Semiconductor or Fiber Lasers

Stéphane Blin, Olivier Vaudel, T. T. Tam, Pascal Besnard, Sophie La Rochelle, Renaud Gabet, Guy Stéphan

Spectral and time phenomena in optical injection using distributed feedback semiconductor or fibre lasers

S. Blin[1], O. Vaudel[1], T.T. Tam[2], P. Besnard[1], S. LaRochelle[3], R. Gabet[4], and G.M. Stéphan[1]

[1]Laboratoire d'Optronique CNRS UMR 6082, GIS FOTON, ENSSAT, 6 rue Kerampont, BP 447, 22305 LANNION CEDEX, FRANCE
[2]Faculty of Technology, Vietnam National University of Hanoi, Cau Giay, HANOI, VIETNAM
[3]COPL, D´epartement de génie électrique et de génie informatique, Université Laval, SAINTE-FOY, QUEBEC G1K 7P4, CANADA
[4]ENST, Département COMELEC, CNRS URA 820, 46 rue Barrault, 75634 PARIS CEDEX 13, FRANCE

Avril 2004

Abstract. Optical injection is compared for distributed feedback semiconductor and fibre lasers whose wavelength is around 1550 nm. A spectral description of an injected semiconductor laser is presented for usual injected power (> 30 dBm), by mapping out several phenomena, such as bistable areas, undamped relaxation and chaos synchronization. For weak injection levels (< 30 dBm), the slave acts as a highquality amplifier of spectrally narrow signals. In this case, the slave frequency is pulled by the master one. Theory of weak injection is demonstrated using a generalized Airy's function method. We also present the temporal response of a fibre laser output power for static injection, and observe original dynamics linked to relaxation processes. A new method using optical injection is proposed to measure narrow linewidth or spontaneous emission rate.

PACS. PACSkey discribing text of that key – PACSkey discribing text of that key

1 Introduction

A few years after the first experimental demonstration of a laser by Maiman, Stover [1] presents an optical injection experiment using gas lasers. The signal of a master laser is seeded into a second laser called the slave, using an optical isolator to assure a unidirectional coupling between the lasers. The first optical injection experiment using semiconductor lasers was presented by Kobayashi [2]in 1980, using 840 nm AlGaAs semiconductor FabryPerot lasers.

The main properties of optical injection occur when the frequencies of both lasers are close together and the injected power is high enough: The slave gets the spectral properties of the master one in terms of frequency and linewidth [3] - [5]. Afterwards, optical injection has been widely used by scientists to obtain tunable, powerful and narrow linewidth lasers for various applications in domains such as telecommunication, spectroscopy or metrology. For example, optical injection is a way to measure α factor [6] [7], to reduce laser noises (frequency [8] [10],partition [11] or intensity [12] noises), to generate microwave signals [13] [18], to obtain an alloptical clock recovery [19] [21], to generate or synchronize chaos [22][26],etc.

If optical injection has been widely studied and applied for gas or semiconductor lasers, that of a fibre laser is not yet well characterized. Until now, fibre lasers are injected to generate chaos [25] [26], or to control their multimodal spectral distribution. In the 90's, improvements of photosensitive and rareearthdoped optical fibres [27] lead to the manufacture of singlemode Distributed FeedBack (DFB) fibre lasers [28]. Nowadays, powerful single-mode and singlepolarization fibre lasers [29] are available, that permits fundamental studies of optical injection.

In this letter, we present the static or quasistatic optical injection of a singlemode DFB fibre laser. The comparison of optical injection experiments using semiconductor or fibre lasers emphasizes multiple differences between those sources, such as linewidth, α factor[1], or relaxation oscillation frequencies. The influence of those differences in optical injection experiments will be presented. Usual optical injection will be first described in the spectral domain using semiconductor lasers, and compared for different natures of the slave: Influence of α factor and relaxation oscillation frequencies will be highlighted. The case of weak

[1] The α factor was introduced by Henry [30]. It traduces the spectral dissymmetry of gain in semiconductor lasers.

injection will demonstrate the influence of the master coherence by both experimental and theoretical ways. Finally, original time dynamics of an optically injected fibre laser will be presented.

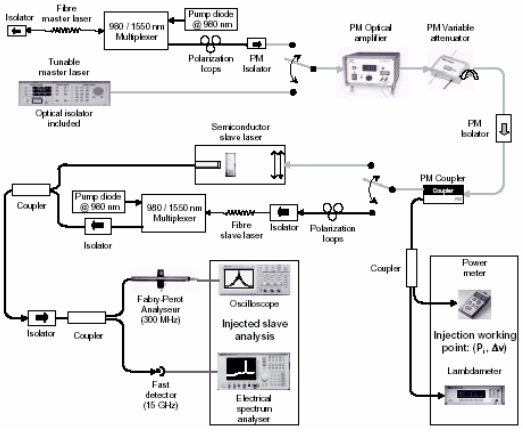

Fig. 1. Experimental setup of optical injection.

2 Usual injection and its spectral properties

2.1 Experimental setup

Figure 1 displays the main sketch of our experiments. All components are pigtailed or fibred components.

The master laser is a single mode tunable semiconductor laser, or an erbium:ytterbium codoped Distributed FeedBack (DFB) fibre laser [29]. Fibre lasers are manufactured at the COPL using a technique similar to that used by Loh [31]. The fibre laser is pumped using a 980 nm semiconductor laser diode, and optically isolated to avoid unstable behaviour due to optical feedback. The Bragg grating that constitutes the fibre laser cavity is an excellent sensor for external perturbations (temperature, pressure, etc.), so that a careful packaging of the laser is necessary to ensure a stable behaviour: The fibre laser is placed in the groove of a copper piece filled with silicon heat sink paste. Master power can be increased up to 18 dBm thanks to an erbiumdoped fiber optical amplifier, but injected power is tuned using a variable optical attenuator in order to maintain a constant signal to noise ratio of the injected signal. In this letter, the property of interest of those master lasers is their coherence: The Full spectral Width at Half Maximum (FWHM) of the semiconductor laser is 125 kHz, that of the fibre laser is 50 kHz. The slave laser is a 1.55 µm massive InP/InGaAsP buried double heterostructure DFB chip, whose linewidth (FWHM) varies between 150 MHz and 8 MHz (depending on the pumping rate); or a fibre laser as presented before.

Semiconductor lasers are linearly polarized, so that a scalar optical injection is obtained thanks to Polarization Maintaining (PM) components: That allows a perfect reproducibility of the experiments. If fibre lasers are singlepolarization ones, their polarization is unknown. As shown on figure 1, the fibre master laser is linearly polarized using a PM isolator, polarization loops are used to maximize the power at the output of the polarizer. Polarization loops are also used before the fibre slave laser to inject the master signal with the same polarization than that of the free slave.

Two different setups are used to injected the master signal into the semiconductor laser. One is used for mappings and provides a 70 dB optical isolation. The other is presented on the figure, and used for weak injections: The master signal is injected using a lens placed at 30 cm far from the slave laser, whose signal is focused into an optical fibre using an optical isolated focuser, so that the isolation of the slave is better than 70 dB.

The control parameters of interest in an injected lasers experiment are the injected power P_{inj} and the detuning $\Delta\nu = \nu_m - \nu_s$ which is the difference between the master frequency (ν_m) and the slave one (ν_s). The pumping rate (r) of the slave is fixed during experiments: It is expressed by the ratio $r = I/I_{th}$ where I is the pumping current, I_{th} the threshold current. The control parameters are monitored using the powermeter and the lambdameter of the master line presented in figure 1. The optical and electrical spectra of the injected slave are observed respectively using a FabryPerot (FP) analyzer and a fast detector coupled to an Electrical Spectrum Analyzer (ESA). The FPs are pigtailed but freespace interferometers with a 135 GHz or 300 MHz free spectral range (finesse is around 100 for both). The bandwidth of the fast detector allows us to observe microwave spectra of the injected laser from 0 to 15 GHz.

2.2 Mapping of optical injection for an injected semiconductor laser

This paragraph introduces the main properties of optical injection that are observed using semiconductor lasers at moderate and high injected powers (> 20dBm). Multiple injection regimes have been described in literature, so that it was essential to dress a map of the injected slave behaviour in a plan defined by the injected power and the detuning. The mapping of the locking area was presented by Mogensen [32] in 1985, then multiple regimes are mapped out, such as relaxation regime [33], chaos [34] and wavemixing [34]. More recently [35] [36], very complete injection maps were obtained, including bistable behaviour [37] [38].

Far from threshold

Figure 2 presents an experimental map of the different injection regimes which are observed for a slave pumped far from threshold, at r = 4. Detuning varies from 60 GHz to +20 GHz, injected power varies from 30 dBm to +8 dBm. The locking area (L) consists into a complete transfer of the spectral properties of the master to the slave (coherence and frequency). The optical spectrum of the nonlinear regime that is wave mixing (1) presents three peaks:

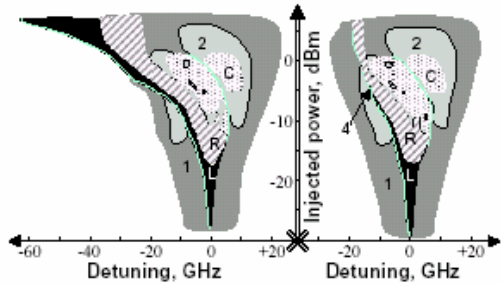

Fig. 2. Experimental map of an injected semiconductor laser far from threshold (r = 4) and its bistable behaviour. The following injection regimes are mapped out: Locking (L), chaos (C), wave mixing (1: single, 2: double, 4: quadruple), and relaxation (R). Left and right maps are obtained respectively for a decreasing and an increasing detuning, both for increasing injected powers.

The main peak is at the free slave frequency νs (without pushing effect[2]), one of the two satellites is at the master frequency νm and the second satellite is the symmetric of νm with respect to νs, usually less powerful. We observe a beating peak at the effective detuning (including pushing effect) with the ESA. The region (2) consists into a doubling phenomenon: Peaks appear on the optical spectrum between the peaks of the single wave mixing (1), a second beating peak appears at the ESA. It is similar for region (4) that arises from region (2): This regime is only observed in a very small part of the map. The relaxation regime (R) looks like wave mixing, but satellite frequencies differ of the slave relaxation oscillation frequency, so that the beating peak do not correspond to the detuning. Note that pushing effect often comes with relaxation. Finally, chaos consists in nonconsistent optical and electrical spectra. Such a generated chaos is well controlled by the injection parameters, offering thus a new scheme for chaos synchronization [40].

Irregularity and lack of symmetry of figure 2 are striking features for moderate and high injected powers (> -20 dBm). The dissymmetry of the map is due to that of the spectral gain, which corresponds to the α factor. Quantification of this dissymmetry is a way to measure this parameter as said in introduction. Another striking point is the bistable behaviour, that was previously observed [41][43]and mapped out [38]. One can observe the wide bistable area (> 40 GHz at Pi = 8 dBm) of the locking area, which is more extended for a decreasing detuning than an increasing one.

Finally, we studied the influence of the polarization of the master laser on the map. We have shown that for an injected master signal whose polarization is perpendicular to that of the free slave, maps are only shifted up of 9 dB: Injected is less effective if polarization of master and slave lasers are different. However, polarization of the locked injected slave remains the same than that of the free slave, that differs polarization locking phenomenon of frequency locking ones.

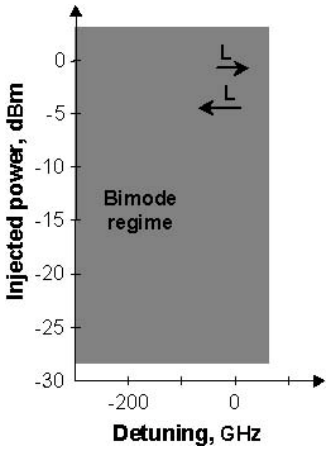

Fig. 3. Experimental map of an injected semiconductor laser close to threshold (r = 1.2) and its bistable behaviour. The striped area corresponds to a locking regime for decreasing detuning only. The map is obtained for increasing injected powers.

Close to threshold

Influence of the pumping rate of the slave laser clearly appears in figure 3, which maps out optical injection for the semiconductor laser that is pumped near threshold, at r = 1.2.

One can observe that nonlinear regimes do not appear at this pumping rate. The slave laser acts as an amplifier as presented by the bimodal regime: Spectral power density of the slave shares in two parts, one at the master frequency, the other at the free slave frequency. A bistable behaviour can also be observe, with a more extended locking area for a decreasing detuning.

In order to compare optical injection using semiconductor or fibre lasers, we mapped out figures 2 & 3 using a master fibre laser instead of the semiconductor one. We did not observed any difference, probably due to the fact that coherences

[2]Pushing effect [39] pushes the slave peak from the free slave frequency far from the master frequency.

of those master lasers are to similar. We persist in thinking that a high coherent master laser should emphasizes nonlinear regimes.

2.3 Mapping of optical injection for an injected fibre laser

In order to compare the behaviour of an injected fibre or semiconductor laser, we study the case of a fibre laser that is injected by the tunable semiconductor laser we used in the last paragraph.

Figure 4 presents the map of the injected fibre laser pumped near threshold at r = 1.7. As previously

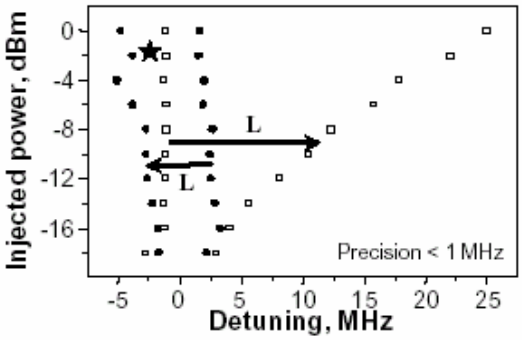

Fig. 4. Mapping of an injected fibre laser at r = 1.7 for an increasing (square) or a decreasing (circles) detuning, both for increasing injected powers.

observed for the semiconductor laser, the map is dissymmetric and provides a bistable behaviour of the locking area. However, the locking area appears here more extended for an increasing detuning, contrary to that of the injected semiconductor laser. Considering that bistable behaviour depends on the α factor, one can ask about amplitude and sign of the α factor of fibre lasers. Note that we also observe bimodal regime as presented for a injected semiconductor laser close to threshold.

Another striking point in this figure is the narrow spectral extent of the map in comparison to that of the semiconductor laser: The injected fibre laser locking area is around 2000 times less extended than that of a semiconductor laser. Such a difference could be explained by the grating strength of the fibre laser that decreases the effective injected power, or the Fabry Perot cavity of the DFB semiconductor laser that allows more resonant frequencies for the injected field than permitted by the grating. Considering the spectral resolution of our FP analyzer around 3 MHz, the frequency jitter of fibre lasers that can reach a few MHz, and the spectral extent of the injection map of 20 MHz, a fine spectral study of the injected fibre lasers is strongly limited.

Finally, note that we tried to observe nonlinear phenomenon by pumping the fibre laser far from threshold and injecting a powerful master signal. We unfortunately did not succeed, probably due to an insufficient injected power.

3 Spectral behaviour of a weak injected laser

This part focuses on spectral characteristics of optical injection, especially coherence phenomena. The main and well known effect is the transfer of master spectral purity (or impurity) to the slave, but such a transfer appears in different manners, depending on the control parameters.

3.1 Weak injection

Weak injection is a linear domain, in comparison to usual injection which exhibits nonlinear regimes such as wave mixing or chaos. Thus a linear domain reveals the phenomenological behaviour of the injected slave laser [44]: A competition occurs between the injected master signal, and the slave spontaneous emission which determines its laser line.

Figure 5 presents the optical injection of a spectrally narrow master signal, at the same frequency than that of the free slave laser. The master is the 125 kHz FWHM semiconductor laser, the slave is a semiconductor laser whose FWHM is 84 MHz. Optical spectra of the injected slave present a pedestal due to the free slave laser, and a spectrally narrow line which corresponds to the amplified master signal as shown on the figure 5 (b). The spectrum observed at a 80 dBm injected power is the free slave spectrum. For higher injection levels, the amplified master component appears and progressively gets all the power of the slave: The transfer of coherence is progressive and leads to a complete locking regime. The amplified master component grows up at the expense of the slave component: That is a competition between the external and the free slave signals. Considering the output power of the injected slave as a constant (injected power is minimum 30 dB less than that of the free slave), the concentration of the power of the slave inside a spectral band which is much more narrow leads to a higher maximum of the spectral density as shown on the figure 5 (a). Moreover, note that the spectral resolution of the FP analyzer is 24 times more than the master linewidth: Amplitude and FWHM of the locking regime spectra are actually limited by the FP resolution.

The behaviour observed in figure 5 (b) leads us to consider the slave as an optical amplifier, whose gain is studied in figure 6. The dependence of the gain vs. the injected power is classic: We observe a small signal gain plateau for injected powers weaker than -45 dBm, then the gain decreases with increasing injected powers due to the saturation of the matter. However, the correlation of figures 6

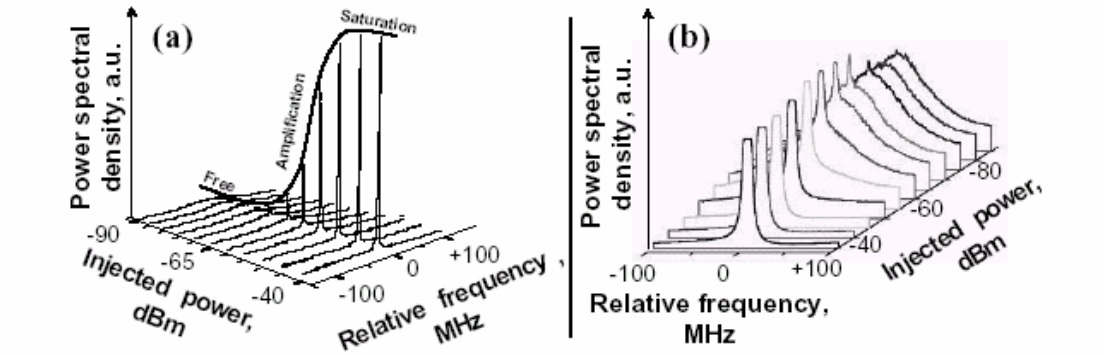

Fig. 5. Amplification of a weak injected signal by the slave laser. (a): Spectra of the injected slave vs. the injected power, at r = 1.4. (b): Truncated spectra of the injected slave in order to focus on the pedestal.

and 5 permits us to define what is the locking regime: The locking regime is the state an injected slave whose gain is saturated by the external injected signal. Such a saturation comes with a complete transfer of coherence: All the power of the slave concentrates into the master spectral band. The small signal gain, around 40 dB, is one decade higher than that of usual semiconductor optical amplifiers. This difference is due to the resonance of the injected field inside the slave, in comparison to a single pass through an optical amplifier. Consequently, if the absolute detuning differs from zero, the injected field

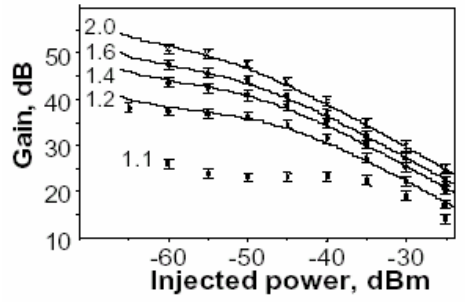

Fig. 6. Gain of the slave vs. injected power at different pumping rates (1.1 to 2.0); points are experimental results, lines come from a generalized Airy's transfer function model.

keeps away from resonance, so that the gain decreases dramatically. Another point is the influence of the slave pumping ratio: The higher is the pumping rate of the slave, the higher is the gain, but the lower is the signal (master component) to noise (slave component) ratio.

Finally, note that this high gain permits us [45] to detect continuous injected powers as weak as -117 dBm. Others used a similar approach to detect weak powers, but using either nonlaser structures [46] - [48] or belowthreshold lasers [49] [50]. Moreover, signal to noise ratio is higher for an upper-threshold laser than an amplifier or a be low-threshold laser, due to the saturation of the main noise that is spontaneous emission (on behalf of the free slave laser line).

3.2 Pulling

The case of a detuned injection clearly presents both the spectral and coherence transfer from the master to the slave. It is the most pedagogical demonstration of the spectral locking phenomenon. We will observe that the slave component frequency of the injected slave spectrum is pulled by the master frequency with increasing injected power. Such a phenomena was predicted by the Adler model [51], but people only observed pushing effect, probably due to an insufficient feedback isolation of their experimental setup that does not permit a weak injection study.

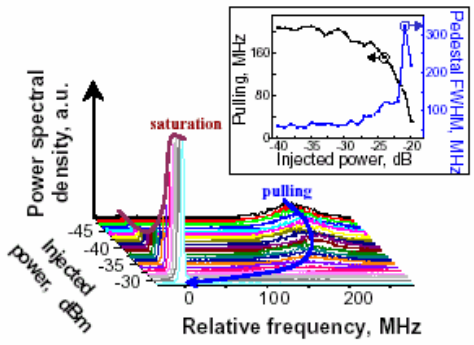

Fig. 7. Evolution of optical spectra vs. injected power for a - 209 MHz detuned injection at r = 1.7. Inset: Frequency pulling and linewidth of the slave component vs. injected power.

Figure 7 presents the optical injection of a spectrally narrow master signal, at a 209 MHz detuning. The master is the semiconductor laser (FWHM of 125 kHz), the FWHM of the free slave is

22 MHz. Optical spectra of the injected slave shown at the figure 7 present two components: One is due to the slave, the other one is the amplified master line. The spectrum observed at a -50 dBm injected power is the free slave spectrum. For higher injection levels, the amplified master component appears and progressively gets all the power from the slave: The transfer of coherence is progressive and leads to a complete locking regime. As presented before, the locking area is defined by the saturation of the gain, that lead on this figure by the plateau at the maximum of the master component. In comparison to figure 5, this saturation appears for higher injected powers, due to the fact that the frequency of the injected signal is not at a resonance of the slave laser cavity.

The inset of figure 7 presents the evolution of the slave component of the injected slave spectra, in terms of frequency and coherence. It is shown that the frequency of the slave is pulled by the master for increasing injected powers. Such a result appears as a physical evidence, but we recently presented its first experimental demonstration [52]. Note that the linewidth of the slave component broadens as the injected power increases, due to the increasing detuned reference that is the master peak.

3.3 Generalized Airy transfer function

Weak injection experiments lead us to understand phenomena involved in optical injection. On that account, the model of the injected laser that uses a generalized Airy transfer function method comes naturally. Such a method has been applied to lasers [53] in order to study their threshold-crossing, and have been then extended to the case of an injected laser [5] [54]. In this paragraph, we briefly present the most simplified form of the model, that is applied to a singlemode semiconductor FabryPerot laser.

This method is based on the transfer function of the laser. That of a FabryPerot filter is wellknown [55], so that one can easily deduce from this function an expression for the laser:

$$y(v)=\frac{S}{\left[1-e^{-L+G}\right]^2+4\cdot e^{-L+G}\cdot\sin^2(\phi/2)} \qquad (1)$$

If this expression can be obtained using a phenomenological approach, it has been also demonstrated [56] from the Maxwell equations. In the last equation, y is the normalized spectral density of the laser, S represents the spontaneous emission spectral density that can be considered as a constant around the laser single mode, *exp (-L)* represents the round-trip losses, G the saturated gain, and ϕ the round-trip phase.

Such a function takes account of the three fundamentals of the laser that are: The resonance traduced by the filtering effect of the cavity through the structure of the function, the stimulated emission through the gain, and the source that is the spontaneous emission.

As presented before, optical injection consists in a competition between the injected field and the slave spontaneous emission, so that the spectral density of the injected slave signal can be expressed as following:

$$y(v)=\frac{S+\eta\cdot y_m(v)}{\left[1-e^{-L+G}\right]^2+4\cdot e^{-L+G}\cdot\sin^2(\phi/2)} \qquad (2)$$

In the last equation, η is the injection efficiency (that corresponds to injected power), y_m is the normalized spectral density of the master signal.

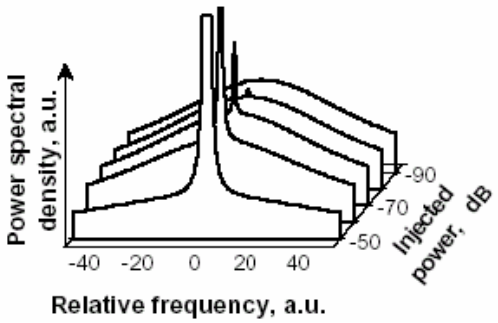

Fig. 8. Theoretical spectra of the injected slave at r = 1.2. Normalized intensity of the injected signal is 21, that of the free slave is 0.2. Master is 100 times more narrow than the free slave.

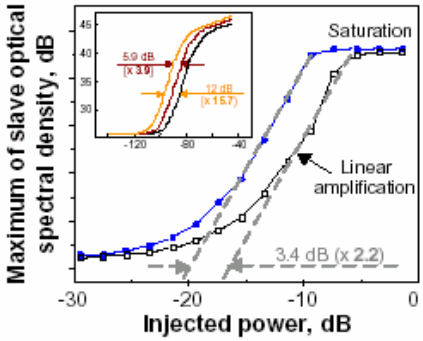

Fig. 9. Experimental and theoretical influence of the master coherence on the maxima of the amplified master component of the injected slave spectra. (a): Experimental results, full circles correspond to a 50 kHz FWHM linewidth fibre master, empty squares to the 125 kHz FWHM semiconductor master; the slave is pumped at r = 1.2. (b): Theoretical results, the left curve corresponds to a normalized linewidth FWHM of 1, the middle one to 4, the right one to 14.

Note that this equation does not lead directly to the theoretical spectra, because y depends on *G* that is

saturated, so that G depends on the normalized power Y (integration of the the spectral density y in the frequency domain). This equation is an integral equation, that can be solve using an analytic method considering simple hypothesis such as a Lorentzian shape of the laser spectra.

Figure 8 presents results obtained using this method. One can observe that shapes of those spectra are in good agreement with those of experiments that are presented in figure 5 (b). Note that the model is also in good qualitative agreement as presented by in figure 6, whose lines correspond to theory and points to experiments.

3.4 Narrow linewidth measurement

One can wonder what is the influence of the master coherence in optical injection experiments. We demonstrate in this letter that, in the weak injection domain, injection is especially efficient since the master laser is coherent, so that we propose an original comparative method to measure the linewidth of a highly coherent laser. Usual methods are based on selfheterodyne detection [57], or inferred from the power spectral density noise: Given that such experiments are limited by technical external perturbations, our alternative solution is of interest. In this paragraph, the master laser is the tunable semiconductor laser or the fibre laser, the slave laser is a semiconductor laser.

The experiment consists in the weak injection of the coherent source signal into the slave. We consider the evolution of the maxima of the injected slave optical spectral density (spectra were presented in fig. 5 (a)) with the injected power. As presented before, the maxima of the amplified master components shown in figure 9 consists in three parts: A plateau at low injected powers corresponds to the free slave regime, the linear part consists in the amplification of the master component in a small signal regime of the slave, the plateau that appears at high injected powers is due to the gain saturation of the slave that defines locking regime. The comparison of this evolution for two lasers whose coherences are different shows that the linear part is shifted by 3.4 dB, i.e. 2.2 in a linear scale, that is directly linked to the 2.5 ratio between the master linewidths.

The inset in figure 9 presents the theoretical results, that agrees with experimental observations: The more coherent the master laser is, the more efficient the injection is. The ratio of 4 (14) between the master linewidths leads to a shift of 5.9 dB (12 dB) of the linear part, i.e. a 3.9 (15.7) factor in linear scale. Note that the resolution of our optical FP analyzer is between the master and the free slave linewidths, so that the saturation level is damped. The effect of the FP analyzer has been introduced in the model, and could be the origin of the small differences between the measured and effective coherence ratios.

Considering the weak injection levels that such an experiment is able to detect, this method should allow us to measure linewidth below 1 Hz with a reference of 100 kHz. Finally, note that the threshold of the linear part presented in figure 9 should offer us a measure of the spontaneous emission rate of the slave laser: Threshold occurs when the injected power and the spontaneous emission of the slave (which leads to the free slave laser line) are similar.

4 Temporal dynamics

Among the differences announced between semiconductor and fibre lasers, one has not been completely highlighted, that is relaxation oscillation frequencies. Those of semiconductor lasers are usually greater than the GHz, those of DFB fibre lasers are usually under 1 MHz. Such a frequency allows a temporal study of optical injection that was difficult using semiconductor lasers considering the bandwidth of standard oscilloscopes. If the study of the spectral characteristics of an injected fibre laser is difficult as presented at section 2.3, the temporal study is easily available.

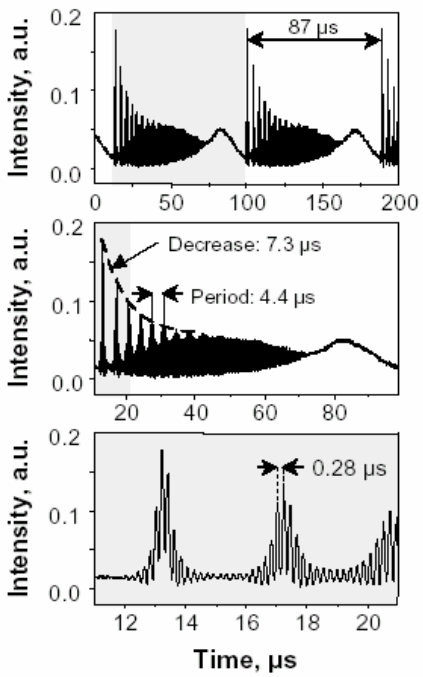

Fig. 10. Temporal behaviour of a fibre laser injected at r = 2 for a negative detuning near the locking area. Detuning is -3 MHz ±3 MHz, injected power is -1.7 dBm. Windows correspond to a same trace is plotted at different scales.

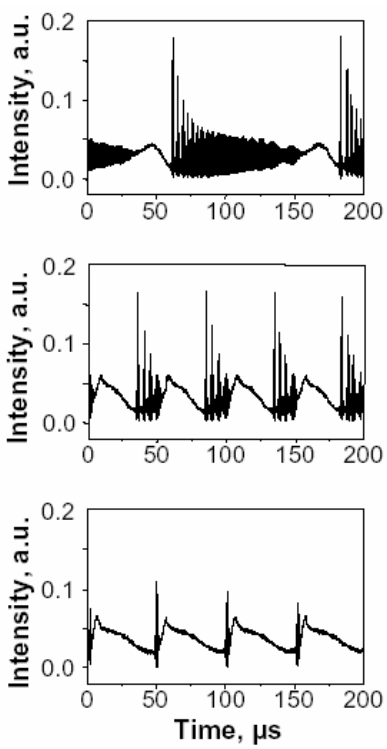

Fig. 11. Temporal dynamics that lead to locking regime of a injected fibre laser injected at r = 2. Graph are obtained at different detunings, that are increasing from up to down. Injected power is -1.7 dBm.

In this section, both master and slave lasers are DFB fibre lasers. Considering the temporal response of the injected slave to an external signal, we observe curious phenomena that are presented for the first time in figure 10. This graph is obtained for an injection working point that is marked by a star on figure 4.

One striking point is the dynamic behaviour of the injected slave, even if it is a static injection (all parameters are fixed). Another surprising point is the multiple structure of this behaviour. The main period of 87 µs (11.5 kHz) appears on the upper graph of figure 10. We can not explain such a phenomenon, that looks like excitability. The middle graph presents classic shape of damped pseudoperiodic spikes that are characteristic of relaxation oscillations, with a period of 4.4 µs (227 kHz) and a decreasing time of 7.3 µs. Finally, the fine structure contains a carrier frequency at 3.7 GHz that could be explained as a beating between the master and the slave components. As shown on the upper graph of figure 10, the slave laser is perturbed by the injected signal, that lead to a relaxation process. However, relaxation processes appear periodic and stable, that is to understood. Note that optical spectra of the injected slave are not available using scanning FP analyzers.

In order to complete the experimental observation of those original dynamics, we describe the evolution of the temporal behaviour with an increasing detuning, at the injected power of -1.7 dBm. At a very negative detuning, the slave is in its freeslave regime so that intensity is continuous. With an increasing negative detuning, the slave amplified progressively the master spectral peak that lead to a bimodal regime. Such a regime is characterized by the beating between slave and master components of the spectra, that induces a carrier in the temporal domain whose frequency and amplitude are respectively determined by detuning and amplitudes of both master and slave components. For an increasing negative detuning greater than -5 MHz, the shape of relaxation processes appears in the beating signal: That is shown on the upper graph of figure 11. Then, main period, amplitude and number of spikes decrease when the injected slave tends to the locking regime that is characterized by a continuous signal. Finally, note that this behaviour has been observed using a fibre laser as a slave, and that it does not depend significantly on the nature of the master laser.

5 Conclusion

In this letter, we have presented optical injection for semiconductor and/or fibre lasers, in order to highlight parameters of influence in optical injection experiments. The main control parameters of optical injection are the injected power, the detuning and the pumping rate of the slave laser.

The study of moderate and high injected powers domain revealed the influence of the master signal polarization on the efficiency of injection. The use of an injected slave fibre laser permits to show that bistable locking areas are situated either at negative or positive detuning, depending on the α factor of the slave. Another parameter of influence that has been highlighted is the relaxation oscillation frequencies of the slave that give the spectral extent of injection maps. Low relaxation of fibre lasers permit a temporal study of optical injection that lead to relaxation oscillation processes observations whose periodic behaviour has not been explained.

The study of weak injection was the way to define that locking regime appears with the saturation of the injected slave gain. We showed that the slave acts as a highgain amplifier for weak injected signals. Weak injection domain also permits to prove the impact of the master coherence on the injection efficiency, and to observe frequency pulling as predicted by Adler. Weak injection studies were supported by a simple and efficient

model based on the generalized Airy function method.

Finally, many methods were called back or proposed using optical injection experiments in order to measure the alpha factor of a fibre laser, crosssaturation coefficients or polarization coefficient gain of the active slave medium, linewidth of a highcoherent master laser, or spontaneous emission rate of the slave laser.

6 Acknowledgments

Authors would like to thanks Isabelle Castonguay and Guillaume Brochu for the manufacturing of fibre lasers.

References

1. H. L. Stover and W. H. Steier, Applied Physics Letters 8, (1966) pp. 91–93.

2. S. Kobayashi and T. Kimura, Electronics Letters 16, (1980) pp. 668–670.

3. L. E. Erikson and A. Szabo, Applied Physics Letters 18, (1971) pp. 433–435.

4. P. Gallion, H. Nakajima, G. Debarge, and C. Chabran, Electronics Letters 21, (1985) pp. 626–628.

5. G. St´ephan, Physical Review A 58, (1998) pp. 2467–2471.

6. R. Hui, A. D'Ottavi, A. Mecozzi, and P. Spano, IEEE Journal of Quantum Electronics 27, (1991) pp. 1688–1695.

7. K. Iiyama, K. Hayashi, and Y. Ida, Optics Letters 17, (1992) pp. 1128–1130.

8. P. Spano, S. Piazzolla, and M. Tamburrini, IEEE Journal of Quantum Electronics 22, (1986) pp. 427–435.

9. N. Schunk and K. Peterman, IEEE Journal of Quantum Electronics 22, (1986) pp. 642–650.

10. O. Lidoyne, P. B. Gallion, C. Chabran, and G. Debarge, IEE Proceedings 137, (1990) pp. 147–153.

11. K. Iwashita and K. Nakagawa, IEEE Journal of Quantum Electronics 18, (1982) pp. 1669–1674.

12. A. Furuzawa, Optics Letters 21, (1996) pp. 2014–2016.

13. S. Kobayashi and T. Kimura, IEEE Transactions on Microwave Theory and Technique 30, (1982) pp. 421–427.

14. L. Noel, D. Marcenac, and D. Wake, Electronics Letters 32, (1996) pp. 1997–1998.

15. J. Genest, M. Chamberland, P. Tremblay, and M. Têtu, IEEE Journal of Quantum Electronics 33, (1997) pp. 989–998.

16. R. P. Braun, G. Grosskopf, D. Rohde, and F. Schmidt, IEEE Photonics Technology Letters 10, (1998) pp. 728–730.

17. M. Brunel, M. Alouini, F. Bretenaker, M. Vallet, O. Emile, and A. LeFloch, Revue de l'Electricit´e et de l'Electronique 1, (2003) pp. 37–41.

18. Y. K. Seo, A. Kim, J. T. Kim, and W. Y. Choi, Microwave and Optical Technology Letters 30, (2001) pp. 369–370.

19. P. E. Barnsley, H. J. Vickes, G. E. Vickens, and D. M. Spirit, IEEE Photonics Technology Letters 3, (1991) pp. 942–945.

20. K. Smith and J. K. Lucek, Electronics Letters 28, (1992) pp. 1814–1815.

21. L. E. Adams, E. S. Kintzer, and J. G. Fujimoto, IEEE Photonics Technology Letters 8, (1996) pp. 55–57.

22. G. D. VanWiggeren and R. Roy, Science 279, (1998) pp. 1198–1200.

23. J. P. Goedgebuer, L. Larger, and H. Porte, Physical Review Letters 80, (1998) pp. 2249–2252.

24. Y. Liu, H. F. Chen, J. M. Liu, P. Davis, and T. Aida, Physical Review A 63, (2001) p. 031802(R).

25. A. Murakami and J. Ohtsubo, Physical Review A 65, (2002) p. 033826.

26. Y. Imai, H. Murukawa, and T. Imoto, Optics Communications 217, (2003) pp. 415–420.

27. L. Dong, W. H. Loh, J. E. Caplen, and J. D. Minelly, Optics Letters 22, (1997) pp. 694–696.

28. J. T. Kringlebotn, J. L. Archambault, L. Reekie, and D. N. Payne, Optics Letters 19, (December 1994) pp. 2101–2103.

29. M. Ibsen, E. Rønnekleiv, G. J. Cowle, M. O. Berendt, O. Hadeler, M. N. Zervas, and R. I. Laming, Summaries of papers presented at the Conference on Lasers and Electro Optics CLEO'99, (1999) pp. 245–246.

30. C. H. Henry, IEEE Journal of Quantum Electronics 18, (1982) pp. 259–264.

31. W. H. Loh and R. I. Laming, Electronics Letters 31, (August 1995) pp. 1440–1442.

32. F. Mogensen, H. Olesen, and G. Jacobsen, IEEE Journal of Quantum Electronics 21, (1985) pp. 784–793.

33. I. Petitbon, P. Gallion, G. Debarge, and C. Chabran, IEEE Journal of Quantum Electronics 24, (1988) pp. 148–154.

34. E.K. Lee and H. Pang, Physical Review A 47, (1993) pp. 736–739.

35. V. Kovanis, T. Simpson, and J. Liu, Applied Physics Letters 67, (1995) pp. 2780–2782.

36. T. B. Simpson, J. M. Liu, K. F. Huang, and K. Tai, Quantum Semiclassical Optics 9, (1997) pp. 765–784.

37. S. Blin, P. Besnard, R. Gabet, and G. Stéphan, Europhysics conference abstract, European Quantum Electronics Conference EQEC 2003 27E, (2003) Postdeadline EP12THU.

38. S. Blin, C. Guignard, P. Besnard, R. Gabet, G. Stéphan, and

M. Bondiou, Comptes Rendus Physique 4, (2003) pp. 687–699.

39. A. Gavrielides, V. Kovanis, P. Varangis, T. Erneux, and T. B. Simpson, Proceedings of the SPIE 2693, (1996) pp. 654–665.

40. C. Guignard, S. Blin, and P. Besnard, Europhysics Conference Abstracts, European Conference on Lasers and ElectroOptics CLEO EUROPE 2003 27E, (2003) Poster EC1M.

41. S. Kobayashi and T. Kimura, IEEE Journal of Quantum Electronics 17, (1981) pp. 681–689.

42. H. Kawaguchi, K. Inoue, T. Matsuoka, and K. Otsuka, IEEE Journal of Quantum Electronics 21, (1985) pp. 1314–1317.

43. M. Bondiou, R. Gabet, P. Besnard, and G. M. Stephan, Proceedings of the international conference on LASERS'97, (1998) pp. 49–54.

44. S. Blin, G. Stéphan, R. Gabet, and P. Besnard, EurophysicsLetters 52, (October 2000) pp. 60–65.

45. R. Gabet, G. M. Stéphan, M. Bondiou, P. Besnard, and D. Kilper, Optics Communications 185, (2000) pp. 109–114.

46. G. Ferrari, M. O. Mewes, F. Schreck, and C. Salomon, Optics Letters 24, (1999) pp. 151–153.

47. J. H. Marquardt, F. C. Cruz, M. Stephens, C. W. Oates, L. W. Hollberg, J. C. Bergquist, D. F. Welch, D. G. Mehuys, and S. Sanders, Proceedings of the SPIE 2834, (1996) pp. 34–40.

48. A. C. Wilson, J. C. Sharpe, C. R. McKenzie, P. J. Manson, and D. M. Warrington, Applied Optics 37, (1998) pp. 4871–4875.

49. K. Magari, H. Kawagushi, K. Oe, and M. Fukuda, IEEE Journal of Quantum Electronics 24, (1988) pp. 2178–2190.

50. F. S. Choa and T. L. Koch, IEEE Journal of Lightwave Technology 9, (1991) pp. 73–83.

51. A. Siegman, Lasers (University Science Books, 1986).

52. S. Blin, G. Stéphan, and P. Besnard, Technical Digest, International Quantum Electronics Conference IQEC'2002, (2002) p. 294.

53. G. Stéphan, Journal of Nonlinear Optical Physics and Material 5, (1996) pp. 551–557.

54. G. Stéphan, Quantum Semiclassical Optics 10, (1998) pp. 849–860.

55. M. Born and E. Wolf, Principles of Optics (Cambridge University Press, 1980).

56. M. Bondiou, R. Gabet, G. St´ephan, and P. Besnard, Quantum Semiclassical Optics 2, (2000) pp. 41–46.

57. T. Okoshi, K. Kikuchi, and A. Nakayama, Electronics Letters 16, (1980) pp. 630–631.